Subject ID: Preference for oral or poster:

Investigations on cracking characteristics of geosynthetic-reinforced asphalt using DIC

Ashray Saxena[1], V. Vinay Kumar[2] and Jorge G. Zornberg[1]

[1] Department of Civil, Architectural and Environmental Engineering, University of Texas at Austin, Austin, Texas, USA
[2] Huesker Inc., Austin, Texas, USA

ABSTRACT

This study aims at investigating the shear resistance of two-layered asphalt specimens, both with and without geosynthetic interlayer, using monotonic cross-shear test and digital image correlation (DIC) technique. The cross-shear test helps in evaluating the performance of asphalt overlays under the shear loading mode that governs the reflection of cracks into structural overlays. The experimental setup replicated real-world conditions, with a weak pavement as the bottom asphalt layer, overlaid by a structural asphalt overlay. An appropriate amount of tack coat and geosynthetic interlayer (in case of reinforced specimen) were placed at the interface of asphalt layers. Digital images were captured at regular intervals during the monotonic cross-shear test. The displacement fields extracted from these images enabled the determination of shear strains within the specimens, facilitating the understanding of crack initiation and propagation phenomena. The deformation data obtained from DIC analysis were validated with vertical deformations measured via linear variable differential transformer (LVDT). A strong correlation of the DIC data with the measured LVDT data was observed. The DIC data indicated that the shear strains were as high as 3.8% in shear zone in the control specimen (CS) as compared to 0.9% in a geosynthetic reinforced specimen after 9 sec of monotonic loading. Overall, the inclusion of geosynthetic interlayer improved the shear resistance of the asphalt overlay by about 5.01 times compared to the unreinforced asphalt overlay.

Keywords: Asphalt; Geosynthetic; DIC; Cross-shear test

1 INTRODUCTION

The propagation of reflective cracks into overlays stands as a significant contributor to the degradation of overlaid asphalt pavements. A commonly employed method for rehabilitating deteriorated pavements involves treating the deteriorated pavements and the subsequent application of hot mixed asphalt overlays (Kumar et al. 2021). However, the movement of the underlying cracked asphalt layer due to shear and tensile stresses, that are developed due to traffic loads and temperature variations, initiates cracks that subsequently propagates into the overlay, and this phenomenon is referred to as reflective cracking (Sudarsanan et al. 2023). The rate at which these cracks propagate depends on the environmental and traffic conditions. Importantly, the concentration of stresses at the leading edge of underlying crack plays a pivotal role in the upward progression of crack from the bottom layer to the overlay. It is worth noting that a comprehensive solution for entirely preventing crack propagation has not yet been determined, limiting the existing options to only delaying the advancement of such cracks. Among the various techniques recommended to effectively delay the occurrence of reflective cracks, the placement of interlayer systems between the pre-existing pavement and the overlay has proven to be the most effective method (Kumar et al. 2021; Sudarsanan et al. 2023). However, the analysis of crack propagation in hot mix asphalt (HMA) mixtures presents a significant challenge due to their inherent heterogeneity. This complexity has posed a barrier to the integration of fracture-mechanics based models into asphalt concrete mixes (Birgisson et al. 2008). The most common approach for predicting crack initiation and propagation in asphalt mixtures relies on sensors like strain gauges and linear variable differential transformers (LVDTs). While these devices are easy to install, they fall short in delivering precise strain measurement in asphalt specimens due to the necessity of predefining their measurement location before testing. To overcome such issues and enhance the understanding of crack propagation process in asphalt mixtures, there is a need for a high resolution full-field measurement

technique (Yi-qiu et al. 2012).

In the recent decade, various studies (Kumar and Saride 2017; Kumar et al. 2021; Wargo et al. 2017) investigated the mechanisms responsible for reducing reflective cracks and enhancing the performance of asphalt overlays. They employed dynamic four-point bending tests in conjunction with digital image correlation to analyze the crack propagation and the corresponding mobilized strains within the specimens. The studies highlighted the effectiveness and relevance of DIC in understanding the cracking resistance of geosynthetic-reinforced asphalt specimens under repeated loading conditions. Recently, Roodi et al. (2023) depicted failure patterns of geosynthetic-reinforced and unreinforced asphalt specimens as observed from their monotonic cross-shear tests. The specimens were subjected to pure shear loading and results indicated that the severity of cracks at peak load (shear strength) was significantly less in reinforced specimens than those observed in the unreinforced specimens, suggesting interlayers delayed the crack initiation in reinforced asphalt specimens.

Digital image correlation (DIC), a non-interferometric optical measurement method pioneered in the 1980s, was developed to aid in identifying and analyzing the heterogeneity within composites and concrete (Romeo 2013). Various researchers (e.g., Hamrat et al. (2016); Kumar and Saride (2017)) utilized the DIC technique to study the flexural cracking behavior of reinforced concrete beams and high-strength fiber concrete subjected to both static and repeated loads. Their investigations revealed the efficacy of DIC in comprehensively capturing strain fields until failure. Moreover, the technique demonstrated its effectiveness under both static and repeated loading conditions by accurately measuring the crack initiation, crack growth patterns, as well as the associated displacement and strain fields. This study aims to investigate the shear resistance and cracking characteristics of two-layered asphalt specimens, with and without geosynthetic interlayer, under direct shear loading mode. While cross-shear laboratory tests on geosynthetic-reinforced and unreinforced asphalt specimens have been conducted in the past (Saxena et al. 2023), this study introduces the utilization of DIC technique to provide a more comprehensive analysis and interpretation of the cross-shear test results.

2 MATERIALS

2.1 Asphalt

In this study, TY-D, a dense graded asphalt mixture was utilized to prepare both the unreinforced (control) and geosynthetic-reinforced asphalt specimens. Fig. 1 shows the particle size distribution of the aggregates used in the preparation of asphalt mixtures, highlighting that the particles were well within the gradation limits specified by TxDOT (2014) for the dense graded asphalt mixture. A performance grade (PG) 64-22 binder was used to prepare the top asphalt layer (depicting overlay) having 4% air void content and bottom asphalt layer (depicting pre-existing asphalt layer) having 7% air void content. The viscosity of the PG 64-22 binder was determined using a rotational viscometer and determined to be 368 cst at 135 °C. The asphalt mixtures at their respective optimum binder content were observed to have an indirect tensile strength of 786 kPa and 589 kPa with respect to 4% and 7% air void contents, respectively.

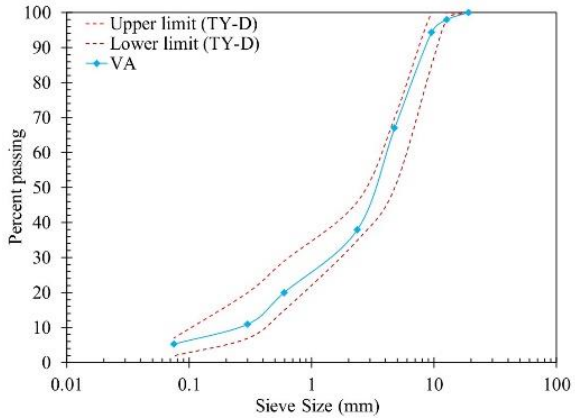

Fig. 1. Particle size distribution of aggregates used in the asphalt concrete mix.

2.2 Geosynthetic Reinforcement

A polyester geogrid composite (PET-C) was adopted as geosynthetic reinforcement in this study, based on its aperture size, bonding capabilities, and mechanical characteristics (Fig. 2). The polyester geogrid composite is manufactured from high modulus polyester yarns and mechanically bonded to an ultralightweight nonwoven polypropylene fabric. The interlayer is completely coated with a binder to enhance the bonding ability with the adjacent asphalt layers. The physical and mechanical properties of geosynthetic adopted in this study are presented in Table 1.

Table 1. Properties of geosynthetic interlayer.

Geosynthetic	Tensile strength (kN/m)	Strain at failure (%)	Aperture size (mm × mm)
Polyester geogrid composite (PET-C)	50 (MD) 50 (CMD)	12	40 × 40

*MD: Machine direction; CMD: Cross-machine direction

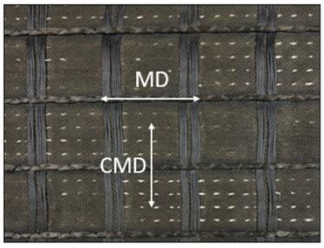

Polyester geogrid composite (PET-C)

Fig. 2. Geosynthetic interlayer adopted in this study.

2.3 Asphalt Specimens

The preparation of unreinforced and geosynthetic-reinforced asphalt specimen for cross-shear tests and digital image correlation analysis involved several distinct stages in the laboratory. Initially, a 57-mm-thick bottom asphalt layer with 7% air void content was compacted via Superpave gyratory compactor in a mold of 150 mm diameter and allowed to cool. Subsequently, a polymerized asphalt cement referred to as AC-15P at rates of 0.27 l/m^2 and 0.54 l/m^2 was respectively used as a tack coat between the unreinforced and geosynthetic-reinforced asphalt layers. A geosynthetic interlayer was then placed (except in unreinforced specimen) and a 57-mm-thick top asphalt layer was compacted with 4% air void content. Higher air void content was chosen for the bottom asphalt layer to represent weak and old pavement layer. Subsequently, the compacted specimens were trimmed into brick-shaped specimens with dimensions of 150 mm (length) × 76 mm (width) × 38 mm (thickness). In the final phase, the brick-shaped specimens were prepared for DIC analysis by initially applying white paint onto their surface. Following this, black paint was sprayed onto the painted white surface under controlled pressure, creating a randomized speckle pattern on the specimen surface (see Fig. 3).

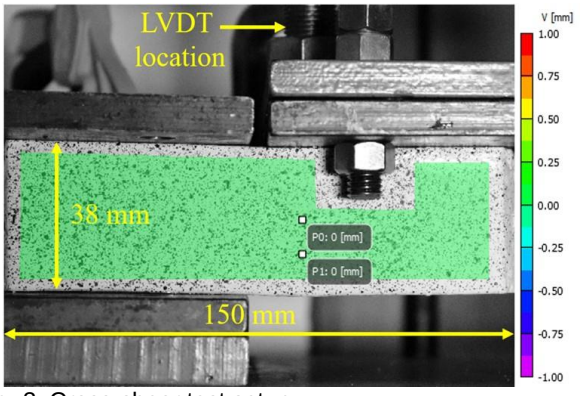

Fig. 3. Cross-shear test setup.

3 TEST METHOD AND ANALYSIS

3.1 Monotonic Cross-Shear Test

Monotonic cross-shear tests were performed on the unreinforced and geosynthetic-reinforced asphalt specimens to understand their shear resistance and the influence of geosynthetic interlayer on the shear/mode II loading performance of the asphalt layers. The cross-shear tests were carried out at room temperature, based on the procedure discussed in Roodi et al. (2023) and Saxena et al. (2023). Monotonic loads were applied on the specimen by applying an initial seating load of 100 N, at a constant displacement rate of 7.68 mm/min. The adopted loading rate was selected based on previous trials, ensuring an acceptable load-displacement response. A load cell was used to measure the load applied on the specimen, while LVDTs were used to measure horizontal and vertical displacements of specimen during shear loading. The load was applied continuously until the specimen fractured completely, i.e. shear resistance became zero. To simulate shear loading on the specimen, the point of load application was strategically situated near the shear plane, specifically 10 mm away from the specimen's center. One of the sides (left side) of the specimen was fixed rigidly while the other side (right side) was subjected to loading (see Fig. 3). Description of the test setup and procedure can be found in Saxena et al. (2023).

3.2 Digital Image Correlation (DIC)

Digital image correlation technique was adopted to analyze high-definition images of the specimen surface, such that the deformations and shear strains in the specimens could be measured during the monotonic cross-shear test. DIC employs optical contactless metrology, which enables measurements that would otherwise be impossible using traditional equipment like strain gauges and displacement transducers. DIC technique has demonstrated success in effectively estimating crack growth in asphalt layers and concrete beams (Kumar and Saride 2017). Within this experimental arrangement, the camera and lens assembly were affixed to an adjustable tripod stand. The tripod's height was adjusted so as to align the lens axis with the specimen front surface. One LED light on a separate tripod was used to ensure consistent lighting on the specimen face. The imaging process involved the use of open software digiCamControl, to focus and continuously record high resolution images of the brick-shaped asphalt specimen with a random speckle pattern. Prior to the test, a calibration image and an undeformed reference image were captured. Subsequently, images were recorded at

regular intervals during the cross-shear tests. VIC-2D, a two-dimensional digital image analysis program, was then employed to calibrate the scale and record track changes in the speckle pattern of deformed images with respect to the undeformed reference image.

4 RESULTS AND DISCUSSION

4.1 Results of Cross-Shear Tests

Fig. 4 presents the cross-shear test results for the two-layered asphalt specimens with and without geosynthetic interlayer in the form of the variation of load resistance with respect to the displacement of specimen. As expected, the control specimen sustained lower loads compared to the reinforced specimen. The peak load values obtained for the specimens evaluated in this study were 2439.59 N (control); and 3288.42 N (PET-C), respectively. Moreover, these load-displacement curves were used to determine the fracture energy (G_D) and fracture energy index (*FEI*) of the specimens with the help of Eq. (1) and (2), respectively. Fracture energy can be defined as the minimum amount of energy required to fracture or crack the two-layered brick-shaped asphalt specimen. While fracture energy index is a dimensionless parameter that combines other HMA fracture parameters, including shear strength, shear strain and fracture energy to characterize the crack resistance potential of two-layered asphalt specimens. The performance of geosynthetic-reinforced asphalt specimen was further evaluated by introducing a non-dimensional performance factor, known as shear strength improvement ratio (SSIR), which is the ratio of fracture energy index of reinforced specimen to fracture energy index of control specimen. The results of the cross-shear tests i.e. fracture energy, fracture energy index, and shear strength improvement ratio for all the tested specimens are summarized in Table 2. It should be noted that to break asphalt specimens more fracture energy is required when geosynthetic interlayer is present in the asphalt specimens compared to that without geosynthetic interlayer (i.e., unreinforced or control specimen). The geosynthetic-reinforced specimen showed the highest cracking resistance potential (fracture energy) of 5442.74 J/m^2. Whereas the control specimen had the lowest fracture energy i.e. 1314.98 J/m^2. The observations made from Fig. 4 and Table 2 suggest that fracture energy increases with the presence of geosynthetic interlayers in the asphalt specimens. This is because the presence of geosynthetic interlayers helps to reduce the rate of reduction in stiffness of the asphalt specimens, which in turn helps in improving the fracture energy of the specimen. It can also be observed from Fig. 4 that after the peak load has reached (i.e. after crack initiation), specimen with geosynthetic interlayer sustained more load compared to control specimen. This may be because, after crack initiation, the response in the post-cracking phase is governed by the elongation at breakage of the reinforcement layer (Roodi et al. 2023). Thus, it can be said that incorporation of interlayer improves the fracture resistance of two-layered asphalt specimens by effectively absorbing the shear stresses that develop under mode II (shear) loading.

$$G_D = \frac{1}{tb}\int f(x)dx \quad (1)$$

$$FEI = \frac{G_D}{t\tau}\gamma \times 10^3 \quad (2)$$

where, G_D = fracture energy; *FEI* = fracture energy index; t = specimen thickness; b = specimen width; τ = shear strength of specimen; γ = shear strain at peak load; and $\int f(x)dx$ = area under the load-displacement curve.

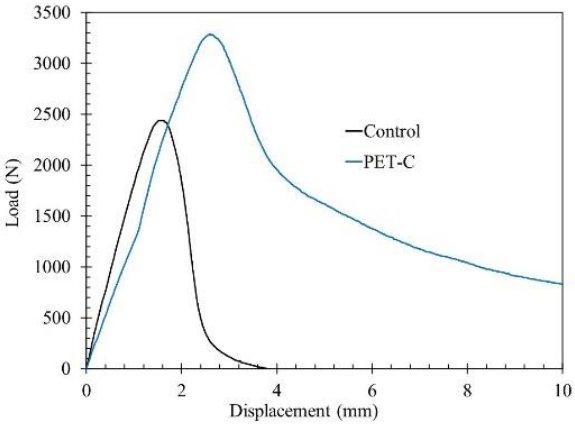

Fig. 4. Load-displacement curves for tested specimens.

Table 2. Cross-shear test results.

Specimen	Fracture energy, G_D (J/m^2)	Fracture energy index (FEI)	Shear strength improvement ratio (SSIR)
CS	1314.98	1.71	---
PET-C	5442.74	8.56	5.01

However, a comprehensive understanding of shear behavior and crack formation under shear loads in asphalt specimens (both with and without geosynthetic interlayer) can be obtained through the use of DIC technique, as described in the subsequent section.

4.1 Results of DIC Analysis

The vertical deflection of the specimen, measured on right side using LVDT at 10 mm away from the center of the specimen (see Fig. 3), was a critical parameter in the cross-shear test.

Moreover, using DIC technique, the displacement fields obtained during the test enabled the determination of vertical deformations at different points on the specimen surface. These deformations can be seen as color coded bands, as shown in Fig. 5, where each band represents a consistent magnitude of vertical deformation within the color band. The negative value represents downward movement of the specimen. Within crack free areas, such as the left side of specimen, the vertical deformation bands were uniform along the depth of the specimen. However, in regions those developed cracks, the color bands exhibit irregularities (with no color band around cracked surfaces).

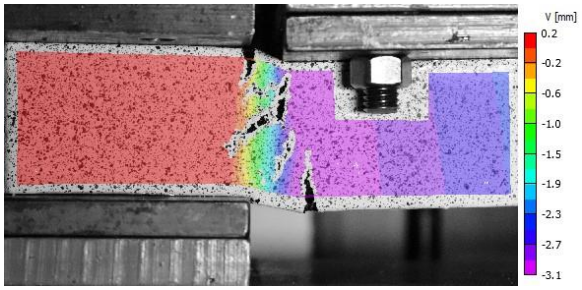

(a)

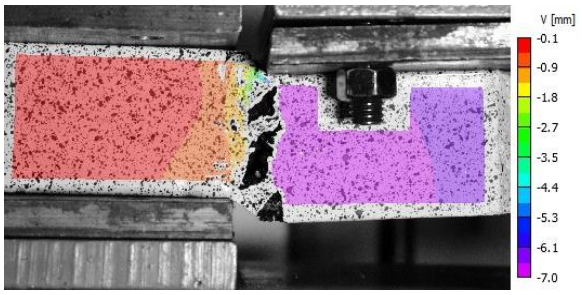

(b)

Fig. 5. Results of DIC analysis showing variation of vertical deformation for two-layered asphalt specimens: (a) CS; (b) PET-C.

During DIC analysis, the vertical deformations were obtained at two locations, P0 and P1 (average out) on the tested specimens (just below the LVDT) through the DIC technique (using VIC-2D) at 10 mm away from the specimen's center and compared against the vertical deformations measured via LVDT at the same location for all the test specimens (see Fig. 3). This comparison is plotted against the loading time, as shown in Fig. 6. The close alignment between the DIC-predicted and LVDT-measured data affirms the reliability and precision of the DIC technique.

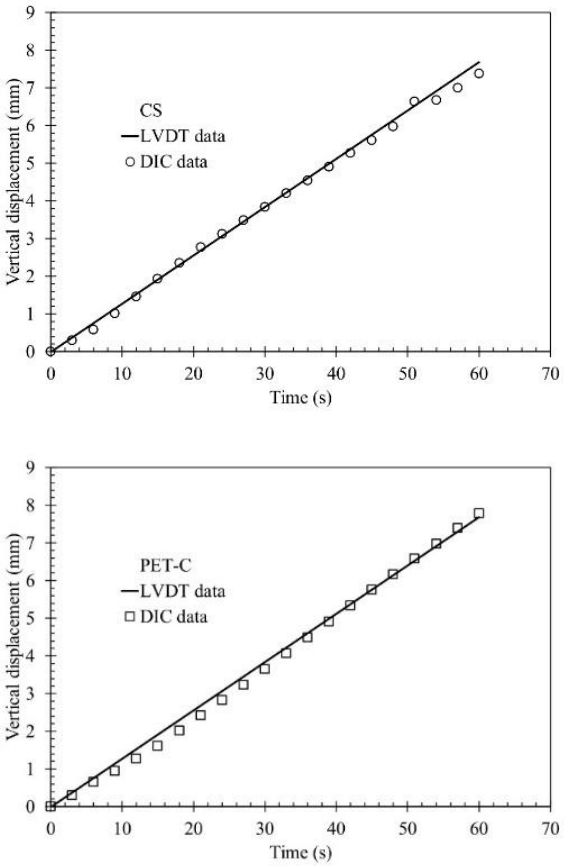

Fig. 6. Comparison of predicted (DIC data) and measured (LVDT data) vertical deformation values.

Furthermore, the analysis of deformation data was conducted to determine the shear strains (ε_{xy}) mobilized within the specimens, aiming to comprehend the initiation and propagation of cracks. Since applied load resulted in shear stresses on the specimens, hence, shear strains were observed within the specimen to evaluate cracking resistance of reinforced and unreinforced specimens. Fig. 7 shows the shear strain contours for specimens with and without geosynthetic interlayer after 9 sec of monotonic loading. This loading time is chosen because after this (i.e. in the next image) crack initiated in control specimen. From Fig. 7, it can be clearly seen that the maximum shear strain (in shear zone, marked with black rectangular box) in geosynthetic-reinforced specimen is 0.9%, while the maximum shear strain in the control specimen is as high as 3.8%. This indicates the presence of geosynthetics in asphalt layers absorbs the shear stresses and delays crack initiation in asphalt overlays under pure shear loading. Similar results can be observed with respect to laboratory testing where geosynthetic specimen performed better than control specimen and higher fracture energy was required to break the reinforced specimen (see Fig. 4). The primary contributor in reducing specimen fracturing is the presence of a geosynthetic interlayer at the

interface zone. This layer absorbs the strain energy resulting from cracks or shear stresses on the specimen, effectively delaying its complete fracture. Fig. 8 shows the shear strain results for tested specimens after 21 sec of monotonic loading. It can be observed from Fig. 8a that high shear strain close to the specimen's top surface (as seen in Fig. 7a) resulted in crack growth from specimen's edge towards center of specimen or from bottom towards center, finally reaching to other edge of specimen. Whereas, in case of geosynthetic-reinforced asphalt layers, the interlayer placed between the old asphalt layer and the overlay absorbed the shear stresses, thus resulted in crack initiation and propagation from the center (i.e. interface location) towards the edge of the specimen. This suggests that higher accumulation of shear stresses near the interlayer might initiate cracks at that location (which is always the weak zone in terms of bond strength), thus resulting in crack propagation from mid-depth (interlayer location) towards edge of specimen.

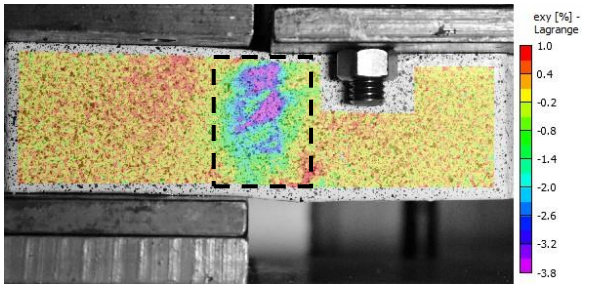

(a)

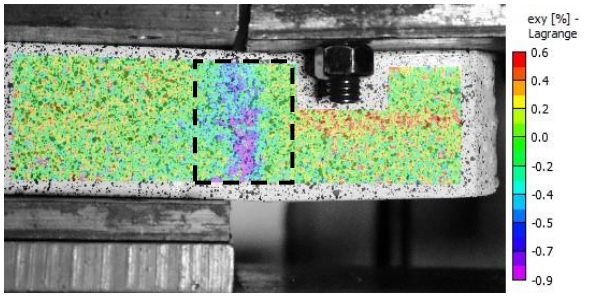

(b)

Fig. 7. Shear strain contours for the tested specimens after 9 sec of loading: (a) CS; (b) PET-C.

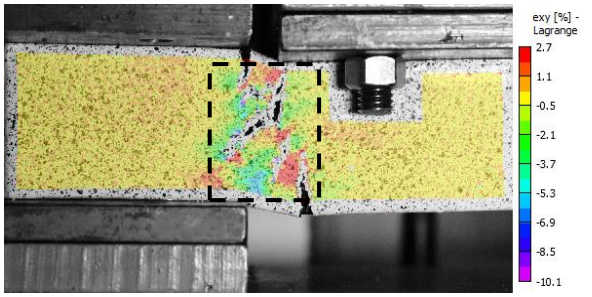

(a)

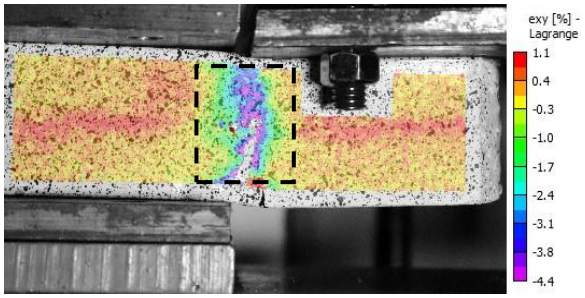

(b)

Fig. 8. Shear strain contours for the tested specimens after 21 sec of loading: (a) CS; (b) PET-C.

5 CONCLUSIONS

The evaluation of crack resistance potential of two-layered asphalt specimens with and without geosynthetic interlayer was performed using cross-shear test, combined with digital imaging techniques. The following conclusions can be drawn from this study:

Geosynthetic interlayer adopted in this study significantly enhanced the cracking resistance potential of asphalt overlays. This enhancement was marked by an increase in the required fracture energy, fracture energy index and shear strength improvement ratio. Specimen incorporating PET-C interlayer exhibited a fracture energy of 5442.74 J/m^2 and fracture energy index of 8.56.

The application of digital image correlation technique effectively illustrated crack propagation patterns and the corresponding shear strains experienced by the specimen during testing. Notably, the reinforced specimen displayed significantly higher mobilization of shear strain compared to that of control specimen. The shear strains were observed to be as high as 3.8% in the control specimens at 9 sec of monotonic loading compared to that of 0.9% in a PET-C reinforced specimen.

Overall, the presence of geosynthetic interlayer in the asphalt specimen improves the cracking resistance potential of asphalt and thus, requires higher fracture energy to completely fracture the specimen.

REFERENCES

Kumar, V.V., Saride, S., and Zornberg, J. G. (2021). Mechanical response of full-scale geosynthetic-reinforced asphalt overlays subjected to repeated loads. Transportation Geotechnics, 30, 100617.

Sudarsanan, N., Zeng, Z. A., and Kim, Y. R. (2023). Laboratory investigation into the crack propagation mechanism of geosynthetic reinforced asphalt concrete using digital image correlation technique. International Journal of Pavement Engineering, 24(1), 2251079.

Birgisson, B., Montepara, A., Romeo, E., Roncella, R., Napier, J. A. L., and Tebaldi, G. (2008). Determination and prediction of crack patterns in hot mix asphalt

(HMA) mixtures. Engineering Fracture Mechanics, 75(3-4), 664-673.

Yi-qiu, T., Lei, Z., Meng, G., and Li-yan, S. (2012). Investigation of the deformation properties of asphalt mixtures with DIC technique. Construction and Building Materials, 37, 581-590.

Kumar, V. V. and Saride, S. (2017). Evaluation of Flexural Fatigue Behavior of Two Layered Asphalt Beams with Geosynthetic Interlayers Using Digital Image Correlation. Proceedings of the Transportation Research Board 96th Annual Meeting, Washington DC, USA, pp. 8-12.

Wargo, A., Safavizadeh, S. A., and Kim, Y. R. (2017). Comparing the performance of fiberglass grid with composite interlayer systems in asphalt concrete. Transportation Research Record, 2631(1), 123-132.

Roodi, G. H., Zornberg, J. G., Yang, L., and Kumar, V. V. (2023). Cross-Shear Test for geosynthetic-reinforced asphalt. Transportation Geotechnics, 38, 100902.

Romeo, E. (2013). Two-dimensional digital image correlation for asphalt mixture characterisation: interest and limitations. Road Materials and Pavement Design, 14(4), 747-763.

Hamrat, M., Boulekbache, B., Chemrouk, M., and Amziane, S. (2016). Flexural cracking behavior of normal strength, high strength and high strength fiber concrete beams, using Digital Image Correlation technique. Construction and Building Materials, 106, 678-692.

Saxena, A., Kumar, V. V., Correia, N. S., and Zornberg, J. G. (2023). Evaluation of Cracking Resistance Potential of Geosynthetic-Reinforced Asphalt Specimens Using Cross-Shear Test. In Airfield and Highway Pavements, pp. 196-208.

TxDOT (2014). Standard Specifications for Construction and Maintenance of Highways, Streets, and Bridges. Texas Department of Transportation (TxDOT), Austin, Texas, USA.